Progress In Electromagnetics Research Letters, Vol. 101, 35–42, 2021

Modified CSRR Based Dual-Band Four-Element MIMO Antenna for 5G Smartphone Communication

Pankaj Jha[1, *], Anubhav Kumar[1], Asok De[2], and Rakesh K. Jain[1]

Abstract—A four-element multiple-input multiple-output (MIMO) antenna based on a modified Complementary Split Ring Resonator (MCSRR) is presented in this paper for dual-band 5G smartphone applications. An inverted L-shaped radiator is used with MCSRR as an open stub in the ground, where MCSRR is responsible for dual operating bands and enhances the impedance matching. The MCSRR as an open stub in the ground plane creates a notch band that minimizes the interference in 5G wireless communication. The four elements of the antenna are placed in such a way that minimum isolation between antenna elements is obtained, 16.5 dB, without any decoupling, whereas more than 20 dB isolation is achieved by using T-shaped decupling. The antenna achieves dual 10 dB bandwidths from 3.40 GHz to 3.625 GHz and from 3.90 GHz to 4.525 GHz. Envelop correlation coefficient (ECC) is extracted from far-field results to analyse the MIMO antenna performance in practical design consideration.

1. INTRODUCTION

Smartphone technology has become an integral part of wireless communication systems, and its applications are increasing significantly as per user demand. 5G technology has a better data rate, faster speed, better transmission capability, and larger channel capacity [1]. The antenna for 5G technology should incorporate all the above-mentioned features; therefore, a MIMO antenna is more preferable than a single element antenna. Designing a MIMO antenna in a limited space with high isolation is a challenging problem, which can be achieved with different decoupling technologies, but it increases the complexity in antenna designing [2]. Therefore, in this paper, simpler decoupling is used to improve the isolation. In literature, researchers have designed several MIMO antennas with and without decoupling structures for smartphone applications. In [3], a MIMO (four-element) antenna is designed without any decoupling along with L-shaped (inverted) radiating elements. The open stub in the ground advances isolation between antenna elements. In [4], an L-shaped feeding radiator is used in a dual-band MIMO antenna, where strips connected with the ground as well as parasitic strips enhance the impedance matching and create dual operating bands. In [5], four T-shaped radiating elements accomplished with ring resonators (open-loop) are used to obtained dual bands where port to port isolation is 15 dB. In [6], four-element F-shaped (Inverted) radiators based on coupled-fed are designed with multiple strips in the ground plane for smartphone applications. In [7], an unequal feed line is used as a radiator where elliptical slots inserted in the ground develop circular polarization in the MIMO antenna. In [8], a metal frame antenna is designed for smartphone applications with four radiating elements, and self-decoupling is achieved. In [9], T-shaped decoupling is used for isolation enhancement where an L-shaped radiator is used for single-band operating frequency.

Received 16 August 2021, Accepted 17 October 2021, Scheduled 9 November 2021

* Corresponding author: Pankaj Jha (pankaj.maahi@gmail.com).

[1] Department of Electronics and Communication Engineering, Shobhit Institute of Engineering & Technology, (Deemed to be University), Meerut, Uttar Pradesh, India. [2] Department of Electronics and Communication Engineering, Delhi Technological University (DTU), New Delhi, India.

As per the literature survey and requirement of the smartphones, a simple decoupling structure is accomplished in the proposed dual-band MIMO (four-port) antenna for 5G communication system. The physical layout of the proposed antenna is selected with the size of existing smartphones like Sony Xperia Z Ultra, Xiaomi Mi Max 3, Samsung Galaxy Mega and Huawei Mate 20 X, etc. The proposed design is optimized on open stub technology in the ground plane which creates a desired notch to avoid the interference between the allotted contiguous bands of 5G communication system.

2. SINGLE ANTENNA DESIGN AND ANALYSIS

The proposed single element antenna with an open stub as defected ground is depicted in Fig. 1(a). The pertaining dimensions of single element antenna are $G_W = 26\,\text{mm}$ and $G_H = 25\,\text{mm}$ which is optimized

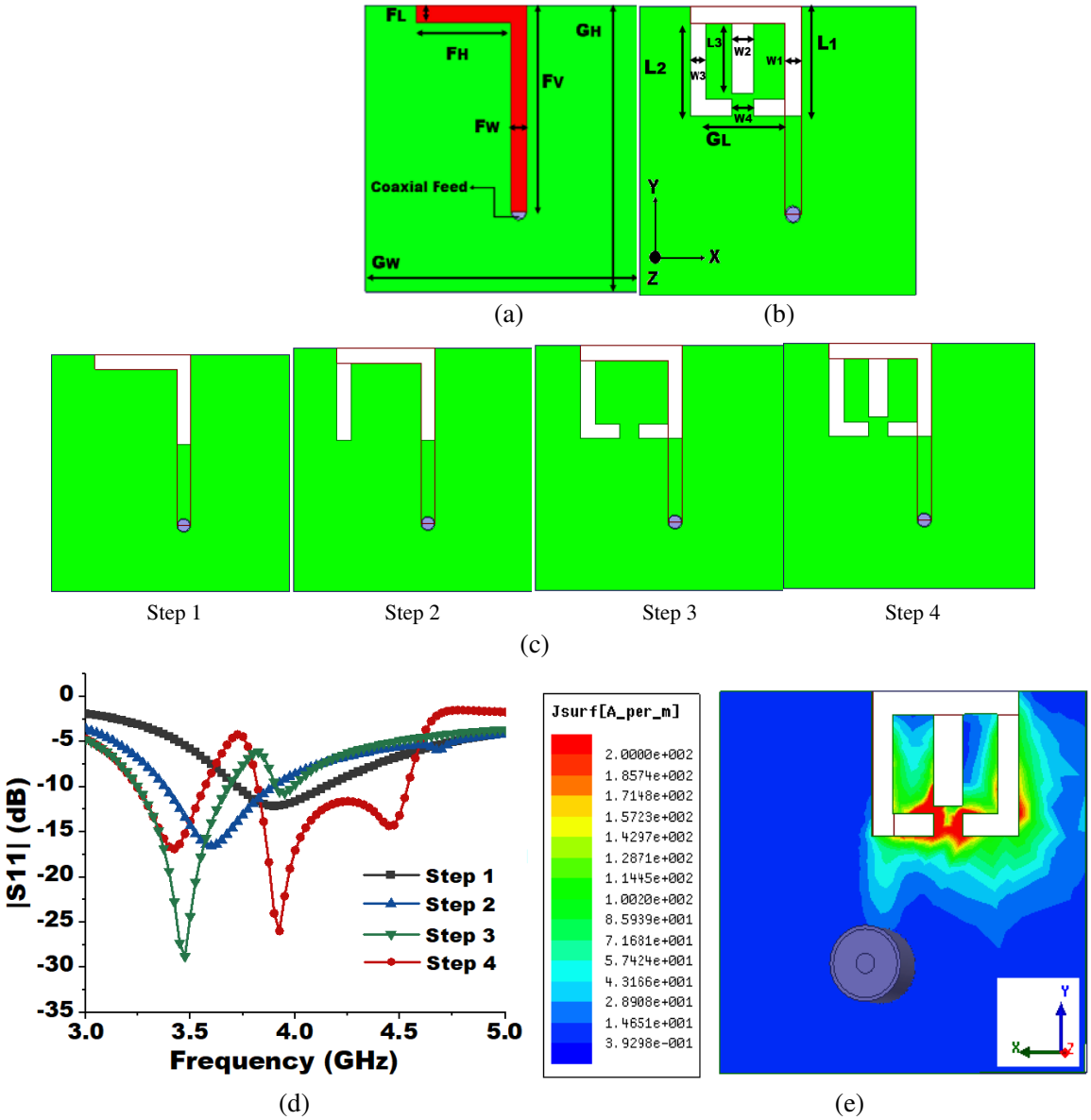

Figure 1. (a), (b) Front and back view of proposed antenna. (c) Single antenna evolution steps. (d) The variations in $|S_{11}|$ associated with all steps. (e) Notch current distribution at 3.725 GHz frequency of the proposed antenna.

on an FR-4 substrate with thickness of 0.8 mm ($\varepsilon_r = 4.4$). An inverted L-shaped radiator is used to design the single antenna element with a 50 Ω SMA connector. The modified SRR with open slot in the ground plane is depicted in Fig. 1(b). The detailed dimensions are $F_L = 1.5$ mm, $F_H = 9$ mm, $F_W = 1.5$ mm, $L_1 = 9$ mm, $W_1 = 1.5$ mm, $L_2 = 6.5$ mm, $F_V = 18$ mm, $W_3 = 0.5$ mm, $G_L = 7.5$ mm, $L_3 = 6$ mm, $W_2 = 2$ mm, and $W_4 = 2$ mm.

The single element antenna is discussed in four steps as depicted in Fig. 1(c) whereas its S-parameter is illustrated in Fig. 1(d). In step 1, an inverted L-shaped radiator is used with an L-shaped open stub in the ground and obtained operating bandwidth (10 dB) varies from 3.725 GHz to 4.125 GHz. In step 2, to improve the impedance matching, another rectangular open stub is incorporated with the existing inverted-L shaped open stub in the ground plane, and impedance bandwidth changes from 3.40 GHz to 3.90 GHz. In step 3, open stubs are altered into CSRR in the ground plane which enhances the bandwidth, and further it creates a notch. The CSRR modifies the lumped parameters, alters the surface current, and creates a notch between the operating band of an antenna in step 2. This notch creates dual operating bands in the antenna which prevent the interference between the two adjacent 5G operating bands (n77 & n78). $|S_{11}|$ in dB varies from 3.275 GHz to 3.675 GHz and 3.925 GHz to 4.0 GHz with a notched band from 3.70 GHz–3.90 GHz. In the fourth step, a rectangular open slot is accomplished in the existing CSRR, and this Modified CSRR (MCSRR) augments the bandwidth of the antenna as well shifting the notch band towards lower frequency. $|S_{11}|$ in dB varies from 3.250 GHz to 3.55 GHz and 3.825 GHz to 4.525 GHz whereas notch is obtained from 3.575 GHz–3.8 GHz frequency.

The frequency of the notch band can be estimated by mathematical Equation (1) [10].

$$f_{\text{notch}} = \frac{c}{((L_{IN} + L_{OT}) - L_{ST})\sqrt{\varepsilon_T}} \tag{1}$$

where L_{IN}, L_{OT}, L_{ST}, and ε_T are given by

$$L_{IN} = (L_1 + L_2 + G_L + W_3) - (W_4 + W_1) \tag{2}$$

$$L_{OT} = (L_1 + L_2 + 2(G_L + W_3) - (W_4) \tag{3}$$

$$L_{ST} = 2(L_3 + W_2) \tag{4}$$

$$\varepsilon_T = \frac{\varepsilon_r + 1}{2} \tag{5}$$

c = light speed and ε_r = Substrate permittivity (relative).

In the proposed design, the values of L_{IN} and L_{OT} are 26 mm and 38 mm, respectively, whereas the value of L_{ST} is 15 mm. The value of ε_r is 4.4 for FR-4 substrate. The calculated value of resonant frequency from the given equation is 3.733 GHz which validates the simulation result. The current distribution (surface) at 3.725 GHz is depicted in Fig. 1(e) which validates the obtained notch band in proposed antenna.

3. DESIGN AND ANALYSIS OF FOUR-ELEMENT ANTENNA

The four single antennae are used to design a MIMO antenna with and without decoupling structure for the smartphone application. The single antenna is placed in smartphone dimension in such a way that the isolation between antenna elements should be maximum without a decoupling structure. To achieve more than 20 dB isolation between antenna elements, a simple T-shaped decoupling is used. The layout design of the four-element dual-band MIMO antenna is completed with the size of smartphones like Sony Xperia Z Ultra, Xiaomi Mi Max 3, Samsung Galaxy Mega, and Huawei Mate 20 X. The overall dimensions of the proposed MIMO are $M_W = 80$ mm and $M_H = 170$ mm. All radiating elements are symmetrically placed at a distance of $G_G = 4$ mm from each corner, and antenna elements 1 and 4 are separated vertically at a distance of $V_D = 44$ mm whereas antenna elements 1 and 2 are separated horizontally at a distance of $H_D = 139$ mm as depicted in Fig. 2(a). The T-shaped decoupling structure in the ground is illustrated in Fig. 2(b). The geometry of T-slots is $A1 = 20$ mm, $A2 = 0.5$ mm, $A3 = 19.5$ mm, and $A4 = 3$ mm. The distances are optimized with $D1 = 34.5$ mm, $D2 = 57$ mm, and $D3 = 42$ mm. The fabricated antenna is illustrated in Fig. 2(c) and Fig. 2(d). The obtained S-parameters without and with decoupling are illustrated in Figs. 2(e) and 2(f), where without any decoupling structure the MIMO antenna achieved 10 dB impedance bandwidth varying from 3.350 GHz

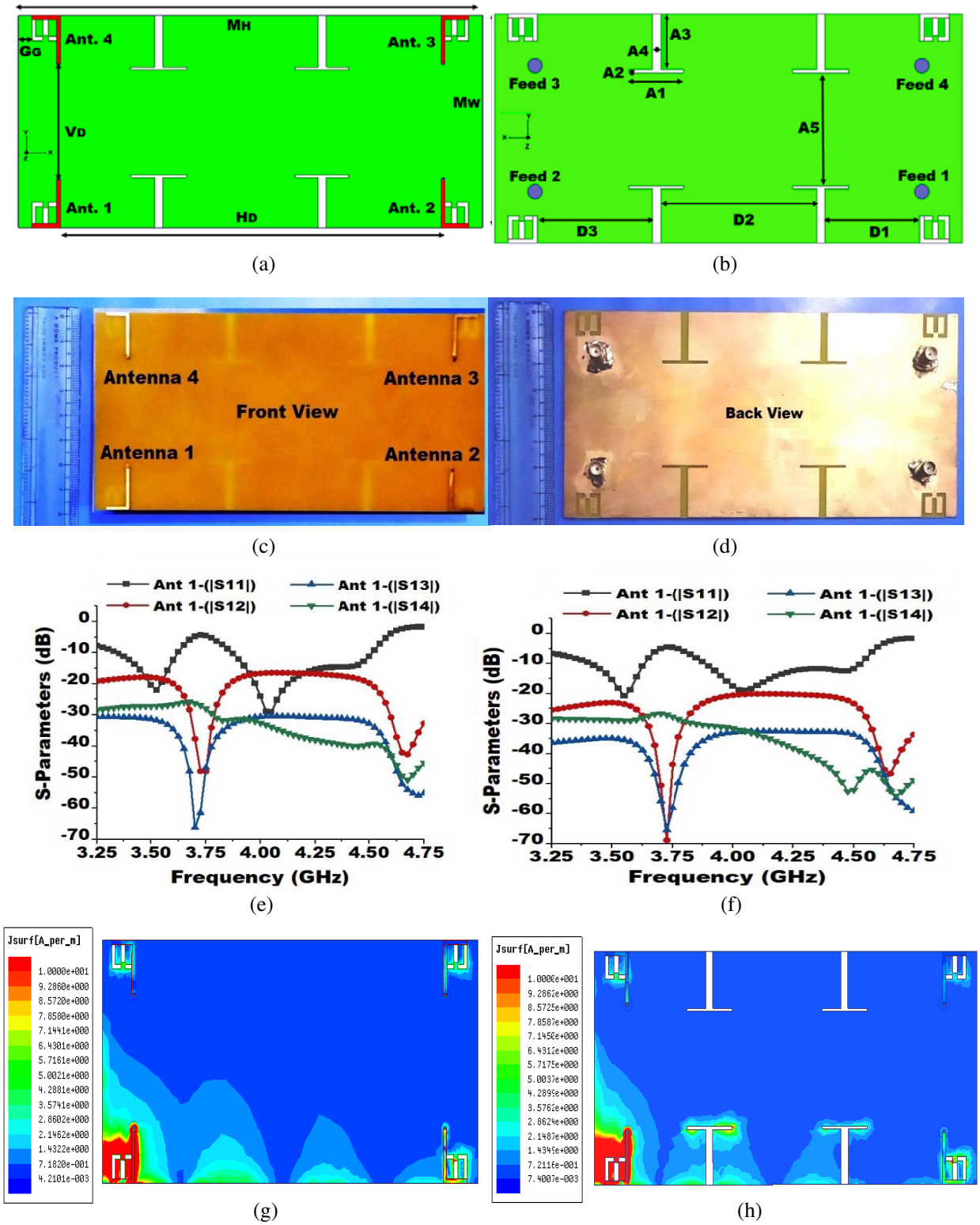

Figure 2. (a) Proposed antenna (top plane), (b) proposed antenna (bottom plane), (c) fabricated antenna (top plane), (d) fabricated antenna (bottom plane), (e) S-parameters without decoupling and (f) S-parameters with decoupling of the proposed antenna, (g), (h) current distribution at 3.55 GHz frequency without decoupling and with T-shaped decoupling.

to 3.60 GHz and 3.875 GHz to 4.50 GHz with notch band from 3.625 GHz to 3.850 GHz. The $|S_{12}|$ changes from 17.880 dB to 19.870 dB in the first operating band and from 16.410 dB to 19.150 dB in the second operating band. To enhance port to port isolation, T-shaped slots are accomplished in the ground which diminish the surface current and improve isolation with maximum value of 8 dB in both operating bands and can be easily accomplished in smartphone without disturbing the MIMO antenna performance. The surface current distributions with and without decoupling are depicted in Figs. 2(g) and 2(h). The proposed MIMO antenna achieved dual operating bands, and 10 dB $|S_{11}|$ varies from 3.40 GHz to 3.625 GHz (partial n77) and from 3.90 GHz–4.55 GHz (partial n78) whereas $|S_{12}|$ diverges from 23.04 dB to 27.33 dB in the first operating band and 20.09 dB to 27.69 dB in the second operating band.

4. RESULT AND DISCUSSION

The proposed dual-band smartphone antenna is simulated by using HFSS-13 EM software and measured using VNA, Anritsu MS2025B. The S-parameters of the antenna are depicted in Fig. 3(a) (simulated and measured)). The simulated value of $|S_{11}|$ in dB varies from 3.400 GHz to 3.625 GHz and 3.90 GHz to 4.525 GHz where it is close to the measured result. The simulated and measured gains (realized)

Table 1. Comparative study of proposed MIMO antenna with recently published work.

Reference	Number of bands	Operating bandwidth (GHz)	ECC	Isolation (dB)	Gain (dB)
[3]	1	1.83–13.82	< 0.018	> 18.8	4.71
[4]	2	3.3–3.6 4.8–5.0	< 0.1	> 16.5	5.1
[5]	2	3.3–3.84 4.61–5.91	< 0.02	> 15	> 4.1
[6]	1	3.6–6	< 0.1	> 10	-
[7]	1	3.4–3.8	< 0.004	> 20	5
[8]	2	0.824–0.96 1.71–2.69	< 0.01	> 14	-
[9]	1	3.4-3.6	< 0.01	> 11	2.1
Proposed work	2	3.40–3.625 3.90–4.55	< 0.3	> 20.1	6.5

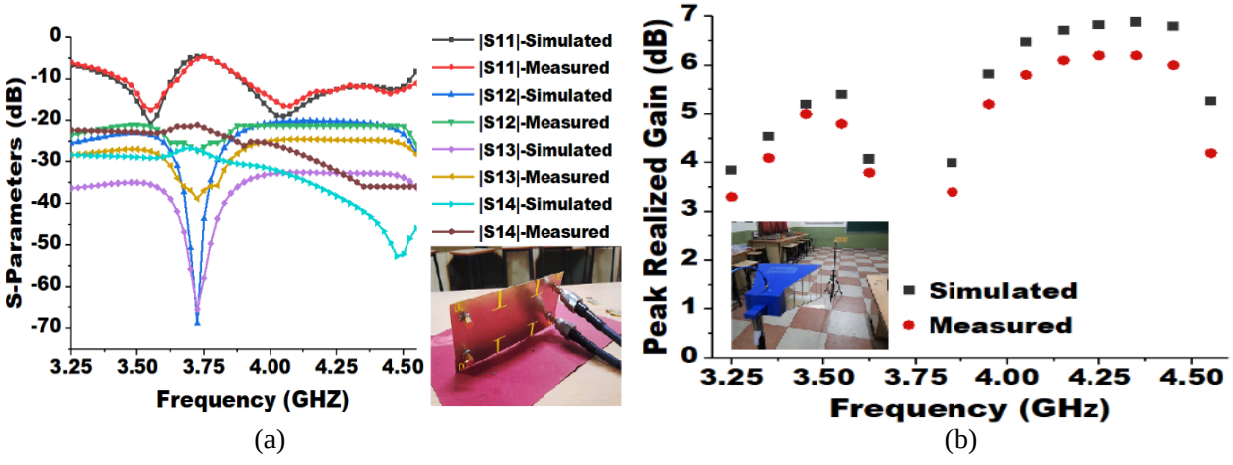

(a) (b)

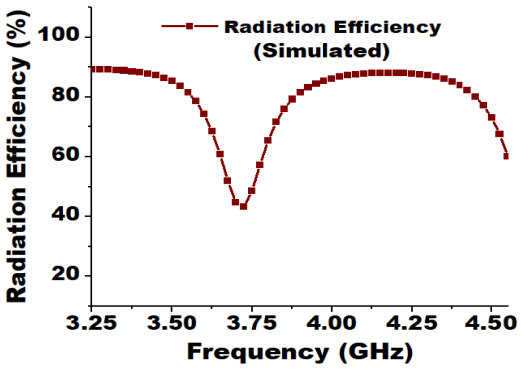

(c)

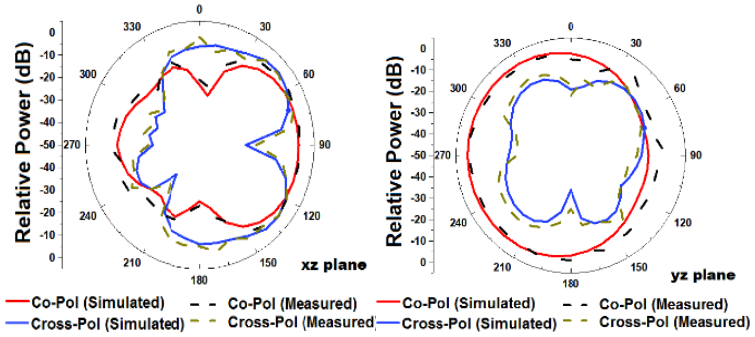

(d)

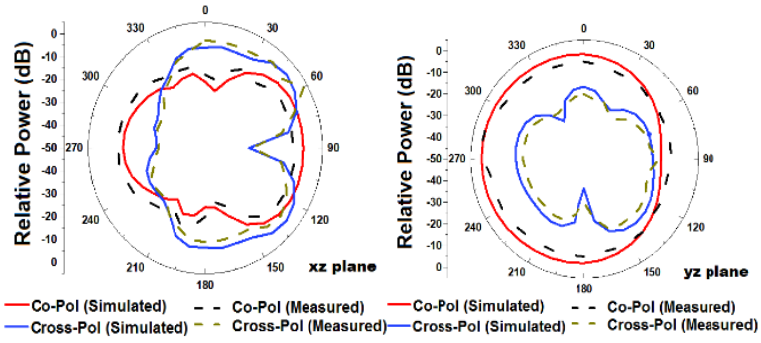

(e)

Figure 3. Simulated and measured (a) S-parameters, (b) peak gain (in dB), (c) simulated radiation efficiency, (d), (e) radiation patterns (normalized) at frequency 3.550 GHz and 4.050 GHz in xz and yz plane.

of the smartphone antenna are illustrated in Fig. 3(b) where the maximum gain is achieved 6.8 dB at 4.250 GHz frequency, and measured peak gain is changing at higher frequencies due to losses associated with free space. Further, the radiation efficiency (%) is more than 81 as depicted in Fig. 3(c). The radiation pattern (normalized) is measured in E-plane and H-plane (xz and yz planes) as illustrated in Figs. 3(d) and (e) at 3.550 GHz and 4.050 GHz centre frequency.

The comparative analysis of the proposed antenna is investigated in Table 1 with other published works, where the proposed antenna has high isolation and low Envelope Correlation Coefficient (ECC) with a simple decoupling structure which is suitable for mobile communication.

5. PERFORMANCE ANALYSIS OF PROPOSED MIMO ANTENNA

MIMO antenna requires low correlation and high isolation for good diversity performance. ECC represents the correlation between radiating elements and how much their radiation patterns affect

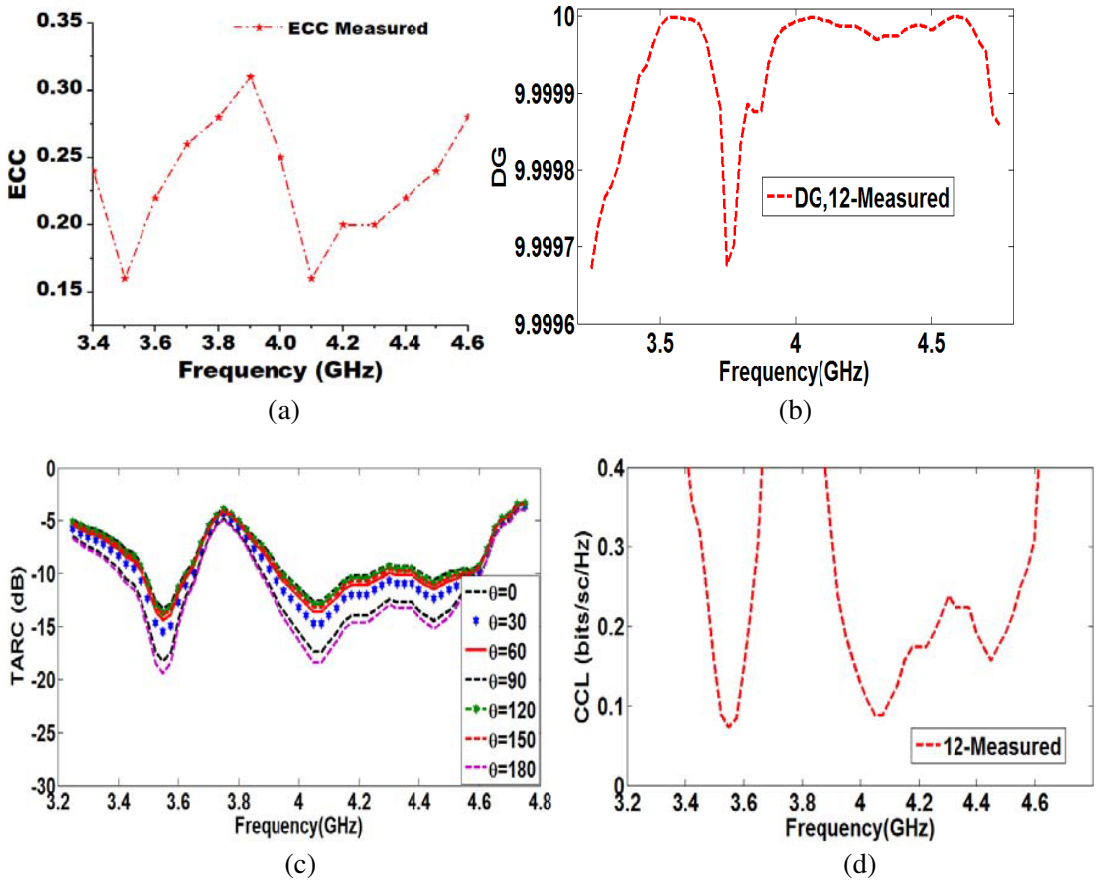

Figure 4. MIMO parameters (a) ECC, (b) DG, (c) TARC, (d) CCL of proposed dual band smartphone antenna.

each other when they are operating simultaneously. Here ECC is estimated using far-field results since MIMO antenna is designed for smartphone applications [12]. The extracted value of ECC is less than 0.3 as depicted in Fig. 4(a) and in permissible limit.

$$\rho_e = \frac{\left|\left({}_0^{2\pi}\int {}_0^{\pi}\int\left(\mathrm{XPR}\,E_{\theta 1}E_{\theta 2}^{*}P_{\theta}+E_{\varphi 1}E_{\varphi 2}^{*}P_{\varphi}\right)\right)\sin\theta d\theta d\varphi\right|^2}{{}_0^{2\pi}\int {}_0^{\pi}\int\left(\mathrm{XPR}\,E_{\theta 1}E_{\theta 1}^{*}P_{\theta}+E_{\varphi 1}E_{\varphi 1}^{*}P_{\varphi}\right)\sin\theta d\theta d\varphi \times {}_0^{2\pi}\int {}_0^{\pi}\int\left(\mathrm{XPR}\,E_{\theta 2}E_{\theta 2}^{*}P_{\theta}+E_{\varphi 2}E_{\varphi 2}^{*}P_{\varphi}\right)\sin\theta d\theta d\varphi} \tag{6}$$

where θ varies from 0° to 180°, and φ varies from 0° to 360°. XPR is the cross discrimination ratio between vertical and horizontal polarized power components, and E_θ and E_φ are the field components, respectively.

The effect of diversity in the communication channel can be analysed with diversity gain (DG), TARC, and CCL which are extracted from measured S-parameters [11]. If channels are less correlated, better signal reception can be obtained through the antenna. A higher value of DG will assure the better performance of the MIMO antenna. The calculated value of DG is close to 10 dB as illustrated in Fig. 4(b).

$$\mathrm{DG} = 10\sqrt{1-|\mathrm{ECC}|^2} \tag{7}$$

To analyze the antenna parameters such as radiation efficiency and bandwidth in a better way, the total active reflection coefficient (TARC) is used. The value of TARC signifies how much power is radiated from the MIMO antenna concerning incident power at a particular phase angle. TARC is calculated

with the help of Equation (8), and it is illustrated in Fig. 4(c).

$$\mathrm{TARC} = \frac{\sqrt{\left(|S_{11} + S_{12}e^{j\theta}|^2 + |S_{22}e^{j\theta} + S_{21}|^2\right)}}{\sqrt{2}} \tag{8}$$

where θ represents the phase angle of input feeding.

The improved channel capacity in a multipath environment results in a higher data rate of MIMO antenna. The channel capacity loss (CCL) is calculated with the help of Equation (9), where ψ represents the correlation matrix. The extracted CCL is illustrated in Fig. 4(d) where it is less than 0.4 bits/sec/Hz and under an acceptable limit.

$$\mathrm{CCL} = -\log_2 \det(\psi^R) \tag{9}$$

6. CONCLUSION

In this paper, a dual-band MIMO antenna (four-element) is discussed, with the help of MCSRR in the ground as an open stub. The MCSRR represents the two characteristics in the ground where it improves the impedance bandwidth of the antenna and provides the notch bandwidth. More than 16.41 dB isolation is achieved between antenna elements without any decoupling and more than 20 dB with simple T-shaped decoupling. The MIMO antenna parameters are analysed to evaluate the antenna performance where ECC and CCL are under acceptable limits, and thus the presented MIMO antenna can be applied to 5G smartphone applications.

REFERENCES

1. Penttinen, J. T. J., *5G Explained: Security and Deployment of Advanced Mobile Communications*, John Wiley & Sons, 2019.
2. Hampton, J. R., *Introduction to MIMO Communications*, Cambridge University Press, 2013.
3. Biswas, A. and V. R. Gupta, "Design and development of low profile MIMO antenna for 5G new radio smartphone applications," *Wirel. Pers. Commun.*, Vol. 111, No. 3, 1695–1706, 2020.
4. Huang, J., et al., "A quad-port dual-band MIMO antenna array for 5G smartphone applications," *Electronics*, Vol. 10, No. 5, 542–547, 2021.
5. Huang, J., G. Dong, Q. Cai, Z. Chen, L. Li, and G. Liu, "Dual-band MIMO antenna for 5G/WLAN mobile terminals," *Micromachines*, Vol. 12, No. 5, 489–495, 2021.
6. Wong, K.-L., Y.-H. Chen, and W.-Y. Li, "Decoupled compact ultra-wideband MIMO antennas covering 3300 $\sim$ 6000 MHz for the fifth-generation mobile and 5 GHz-WLAN operations in the future smartphone," *Microwave and Optical Technology Letters*, Vol. 60, No. 10, 2345, 2018.
7. Chakraborty, S., et al., "A 4-element MIMO antenna with orthogonal circular polarization for sub-6 GHz 5G cellular applications," *SN Applied Sciences*, Vol. 2, 1, 2020.
8. Wong, K.-L., C.-C. Wan, and L.-Y. Chen, "Self-decoupled compact metal-frame LTE MIMO antennas for the smartphone," *Microwave and Optical Technology Letters*, Vol. 60, No. 5, 2018.
9. Ullah, R., S. Ullah, B. Kamal, and R. Ullah, "A four-port multiple input multiple output (MIMO) antenna for future 5G smartphone applications," *2019 International Conference on Electrical, Communication, and Computer Engineering (ICECCE)*, 1–5, IEEE, 2019.
10. Tang, M.-C., S. Xiao, T. Deng, D. Wang, J. Guan, B. Wang, and G.-D. Ge, "Compact UWB antenna with multiple band-notches for WiMAX and WLAN," *IEEE Transactions on Antennas and Propagation*, Vol. 59, No. 4, 1372, 2011.
11. Kumar, A., "Compact 4 $\times$ 4 CPW-fed MIMO antenna with Wi-Fi and WLAN notch for UWB applications," *Radio Electronics and Communications Systems*, Vol. 64, No. 2, 92, 2021.
12. Elshirkasi, A. M., A. A. Al-Hadi, M. F. Mansor, R. Khan, and P. J. Soh, "Envelope correlation coefficient of a two-Port MIMO terminal antenna under uniform and Gaussian angular power spectrum with user's hand effect," *Progress In Electromagnetics Research C*, Vol. 92, 123–136, 2019.